IJCRT.ORG ISSN : 2320-2882

INTERNATIONAL JOURNAL OF CREATIVE RESEARCH THOUGHTS (IJCRT)

An International Open Access, Peer-reviewed, Refereed Journal

A Hybrid Algorithm Integrationwith Regression Methods For Face Recognition

Shaik Sadaf Tabassum (Author)

B Tech (IT) Student, Department of IT

G. Naraynamma Institute of Technology and Sciences, Hyderabad, India

***Abstract*— Humans** excel at face recognition, the challenges of automatic facial recognition persist, particularly in scenarios involving aging, partial occlusion, and facial expressions. This paper proposes a novel face recognition framework comprising three key phases: Pre-Processing, Feature Extraction, and Classification. In the Pre-Processing phase, we enhance contrast and convert RGB images to Grey Level to improve the quality of facial images. Feature extraction involves capturing shape and texture using Active Appearance Models (AAM). The subsequent Classification phase employs an optimized LCDRC model. The pivotal component in the LCDRC model is the projection matrix, which plays a crucial role in enhancing recognition accuracy. To address this, we introduce a new hybrid algorithm known as the Combined Whale Lion Model (CWLM). The performance of our proposed model is evaluated based on metrics such as Accuracy, False Positive Rate (FPR), and False Discovery Rate (FDR). Comparative analysis is conducted against other methods, including LC-DRC, LCDRC-WOA, and LCDRC-CEWO.

Keywords - Face Recognition; AAM Based Feature Extraction; LCDRC Based Classification; LA and WOA; Proposed Model.

I. INTRODUCTION

Over the past two decades, the Biometric-based techniques are emerging as a promising solution for individual recognition. Instead of confirming people's identity and permitting them to entrance to physical and virtual domain based on passwords, PINs, smart cards, plastic cards, tokens, keys and so, It is good to examine the individual's physiological and/or behavioural characteristics that do not change. The password or pin-based approaches are complex to memorize and they can be stolen easily. However, an individual's natal personality can never be misplaced, elapsed, stolen or faked [1][9][10][11]. Thus, the face recognition is one of the interesting as well as important research in the field of biometric recognition. Due to the presence of human activity across a range of security applications, it has attracted significant interest from researchers like airport, criminal detection, face tracking, forensic etc.

The face recognition is the act of recognizing a previously perceived entity as an acknowledged or unfamiliar face. The problem of face recognition is often confused with the Face detection. The face recognition makes a decision if the "face" is somebody well-known, or strange, by means of using a database of faces to authenticate the input face [12] [13] [14] [15]. Till now, two predominant approaches are being deployed to solve the face recognition problem: photometric (view based) and Geometric (feature based). In the Geometric recognition approach, the face's geometrical characteristics, such as the eyes, nose and mouth are first located and thereafter faces are categorized based on a range of geometrical distances and angles between features [16][17] [18] [22]. On the other hand, in the Photometric stereo aids in recovering the outline of an entity from numerous images collected under dissimilar illumination circumstance [23] [24][25].

II. LITERATURE REVIEW

A. Related works

In 2020, Ran He et al. [1] modelled a high-resolution heterogeneity face synthesizing as a complementing union of two elements: a texture in painting element and a posture adjustment element. The two halves are combined into an end to end deep network via a warping method. To enhance visual quality, a wavelet and fine-grained discriminator are used. To guarantee synthesis outcomes, unique 3-dimensional posture correction reduction, 2 adversarial reductions, and an image failure are imposed.

In 2020, Feng Liu et al. [2] present a combined face align and 3- dimensional face regeneration approach for 2- dimensional face photos of random positions and expressions, to concurrently handle these two issues. This technique uses two cascaded regressors sequentially and alternately, one for upgrading two dimensional landmarks and another for three-dimensional face shape, based on a summing theory of three-dimensional face shapes and cascaded regression in two dimensional and three-dimensional face shape spaces.

In 2022, Chaoyou Fu et al. [3] introduced a HFR using a unique Dual variation generation framework and formulate it as a twofold generation issue. To acquire the joint probability distribution of matched heterogeneous pictures, an intricate dual variation generator is used. Yet, the identity variety of sampling may be constrained by the small scale coupled heterogeneous training data. The suggested technique including a wealth of identifying information, which are from large scale observable evidence into joint distribution to get around the restriction.

In 2021, Mandi Luo et al. [4] introduced a face augmentation generative adversarial Network to lessen the impact of uneven deformable feature patterns. The unique hierarchical disassociation module was used to isolate these features from the identification model. In order to ensure the conservation of identifiers in face data augmentation, GCN are also used to recover spatial information by examining the relationships among local areas.

In 2022, Jian Zhao et al. [5] proposed a deep AIM for face identification in the field with three unique features. In order to do cross age face synthesizing and recognition in a way that boosts both processes, AIM first introduces a revolutionary unified deep learning model. Second, AIM avoids the need for coupled data and the actual test samples, achieving continual face aging with outstanding realistic and identity similarity qualities. Third, age invariant facial models completely disentangled from the aging variability are produced by end to end training of the entire deep architecture using effective and unique training procedures.

In 2020, Jin Chen et al. [6] proposing suggested an identity-aware facial mega network to retrieve personal information from LR faces. The magnitude and direction of characteristics that project identify characteristics to a more space is deliberately decomposed into two opposing components in order to acquire identity aware traits successfully.

In 2020, Jae Young Choi and Bum Shik Lee [7] developed a revolutionary GDCNN approach for successfully applying various and numerous Gabor facial models as data during the learning phase of a DCNN for FR purposes. The two main features of the new GDCNN ensemble method are GDCNN building and GDCNN groups. Building GDCNN each learnt with a specific kind of Gabor face expression.

In 2020, Hao Yang and Xiaofeng Han [8] created a facial recognition system depends on real time graphics processing. This paper mainly aims to set cardinal quadrants to face some problems: the face recognition truancy rate with real time video computation, the consistency of the system with video clip processing, the accuracy of the system during actual visit, and the connection configurations of the device with real time video refining.

TABLE I. FEATURES AND CHALLENGES OF EXISTING FACE RECOGNITION APPROACH

Author [citation]	Methodology	Features	Challenges
He *et al*. [1]	WCNN	✓ Reduces the error rate ✓ Reduce the modality difference	× Prone to over-fitting on small-scale datasets
Deng *et al*. [2]	APA	✓ Reduce facial geometric variations ✓ Reducing information loss	× Requires improvement in recognition accuracy × Require more time to train the network
Mocanu*et al*. [3]	DEEP-SEE FACE	✓ Minimize the required computational resources ✓ Training process is quite efficient	× Low accuracy × Extensive Computational time
Iqbal *et al*. [4]	hybrid angularly discriminative features	✓ Consume less relegation power for feature discrimination.	× Training data is relatively small
Zhou *et al*. [5]	EDA	✓ Mining forceful and differentiate features beneath unrestrained illumination situation	× Classification accuracy need to be increased
Zhou *et al*. [6]	WT-LLE-LSSVM	✓ Improves the accuracy ✓ Has stronger robustness to luminosity alteration	× Need to minimize the TRC
Zhou *et al*. [7]	LBP and 2DLPP	✓ Has better sturdiness for a variety of illumination, facial language, and gait and with glasses or not.	× Cannot decrease the inconsistent lighting effects. × Higher training and testing time
Alrjebi*et al*. [8]	2D–MTLBP-F	✓ Enhance recognition accuracy	× Reducing the detrimental impacts of noise, blur, or lighting

III. FACE RECOGNITION: ARCHITYPE AND ITS DESCRIPTION

Here, a unique face recognition method is created by going through the following three stages: **Preprocessing, Feature Extraction and Classification.** Fig. 1 shows a diagrammatic depiction of the suggested facial recognition method. The following list of stages describes how face recognition works:

Step 1: Preprocessing is first applied to the obtained face picture. In the preprocessing stage, the RGB to gray scale conversion and contrast enhancement is undergone.

Step 2: The pre-processed image is Im_{pre}, from which the features are extracted using AAM.

Step 3: Subsequently, these extracted features F are classified using LCDRC model.

Step 4: The projection matrix, which is multiplied with the characteristics throughout the classification process, is the LCDRC classifier's most crucial assessment.

Step 5: In order to improve the recognition accuracy, the projection matrix must be improved. A unique hybrid algorithm called CWLM, which is an extension of the conventional LA and WOA, is presented.

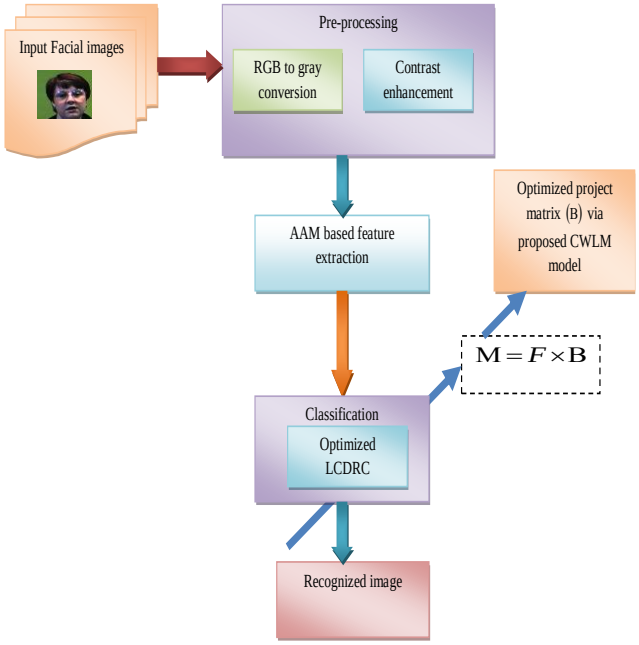

Fig.1. Architecture of proposed Face recognition model

A. Pre-processing

The pre-processing stage is the first and helps to enhance the image's aesthetic appeal. There are two main methods for image processing: Grayscale conversion from RGB with contrast boosting. Initially, all collected input facial image Im_{in} is read using the function $read()$ .This image is transformed into a gray scale image using RGB to gray scale conversion.

RGB to Grey Level Conversion [30]: Typically, aRGB image makes use of no color map and it is represented on the basis of three colour components: red, green, and blue. Such that, Converting RGB to Grayscale for Grayscale Image Pre-processing is crucial. Here, the luminance of the grayscale image is matched with the lluminance of the color image. The gamma expansion is initially used to encode the three main of. The gamma expansion is defined mathematically by Eq (1).

$$E_{linear} = \begin{cases} \dfrac{E_{RGB}}{12.92} & E_{rgb} \le 0.04045 \\ \dfrac{(E_{RGB} + 0.065)}{1.065} & E_{rgb} > 0.04045 \end{cases} \quad (1)$$

In which, E_{RGB} → RGB primitives in [0, 1] and E_{linear} →linear-intensity valuein [0, 1]. Further, the output luminance is acquired using weighted sum of the three linear intensity values. The transformation mechanism of RGB to gray $(\mathrm{Im}_{gray})$is obtained using Eq. (2).

$$\mathrm{Im}_{gray} = f(\mathrm{Im}_{in}) \quad (2)$$

The function $f(\mathrm{Im}_{gray})$achieves this conversion on the basis of the intensity of the three primary colours. This is mathematically expressed in Eq. (3).

$$f(\mathrm{Im}_{gray}) = 0.2989 * R + 0.5870 * G + 0.1140 * B \quad (3)$$

The resultant gray image Im_{gray} is passed to the contrast enhancement phase for enriching the transparency and the visibility of the image.

Contrast enhancement (Im_C)**:** The image values of Im_{gray} are low contrast, such that the contrast enhancement [29] aids in stretching the intensity of the pixels. The contrast is highly enhanced by adopting relative darkness and brightness of R , which is expressed in Eq. (4).

$$\mathrm{Im}_C \to c = \begin{pmatrix} (((R - low\_in)/(high\_in - low\_in))^{\wedge} gamma) \\ * (high\_out - low\_out) \end{pmatrix} + low\_out \quad (4)$$

Here, c →contrast enhancement of R , low_in and $high\_in$ →bounds of the supplied image's contrast and low_out and $high\_out$ →boundaries of the generated image's contrast.

From the acquired contrast enhanced pixel Im_C , the AAM features are extracted.

IV. AAM BASED FEATURE EXTRACTION AND OPTIMIZED LCDRC BASED CLASSIFICATION: A BRIEF OVERVIEW

A. Feature Extraction with AAM

Here, the form and look of face characteristics are extracted using the computer vision algorithm AAM [31].Finding the landmark points is usually how the form and look of the face features are extracted. That define the form and the texture of things that are statistically modelled in the face picture automatically.

Shape Model: It is a consistent geometric form of data that applies to the whole image class.The shape model is logically specified by Eq. (6), where the nk vector represents the shape given by n landmark points in k dimensions of space. In 2D images, n landmarks $\{(Y_j, Z_j): j = 1,2,.....n\}$ define $2n$ vector $(k = 2)$ as in Eq. (5).

$$Y = (Y_1, Z_1, Y_2, Z_2, ..., Y_n, Z_n)^T \quad (5)$$

In order to achieve the statistical validity, it is essential to have all the shape of the in the equivalent referential space. Further to localize all the shapes in a common frame, the GPA is performed after neglecting the location, scale and rotation effects. The aligning sequential pairs corresponding to the shape are extracted with the mean shape. This mechanism is accomplished till there occurs no significant modifications in the iterations. The re-computation of the aligned shape in GPA is expressed mathematically as per Eq. (6).

$$\bar{Y}_k = \frac{1}{N}\sum_{j=1}^{j=N} Y_j \quad (6)$$

The PCA is then deployed on the extracted shape features in order to lessen the data dimensions. This is accomplished by means of exploring the data direction with highest varianceof data and putting the information on the direction. Further, each point Y_j of the data is computed as the sum of the mean and orthogonal linear transformation. Here, $\bar{Y}$ is the mean shape vector and ϕ_j are the shape parameters. The shape features extracted are denoted as f_{shape}.

$$Y_j = \bar{Y} + \sum_{j=1}^{t} \phi_j b_j \quad (7)$$

Appearance Model: The construction of the appearance is based on the intensities of the pixels crosswisethe target image modeled entity. The color channels must be wrapped in the statistical appearance model's design, and the control points are linked to the mean shape. For the purpose of matching the texture, the piecewise affine warping is finished. Further, by means of employing the PCA to texture features, the appearance model $A(Y)$ is acquired. This is expressed mathematically in Eq. (8).

$$A(Y) = A_0(Y) + \sum_{j=1}^{m} \delta_j A_j(Y) \quad (8)$$

Here, A_0 → mean appearance vectors

δ → appearance parameters

$A_j(Y)$ → affine warping-derived synthetic appearance vectors

A extracted appearance parameter is denoted as $f_{apperance}$. The extracted shape and texture features are together represented as $F = f_{apperance} + f_{shape}$.

Optimized LCDRC [26] based Classification

$(F)$is the extracted feature which are subjected to classification via optimized LCDRC classifier, in which the facial images are recognized from the training images. The training matrix o the facial image is expressed in matrix form as $F = [F_1, ...F_2, ...F_c] \in \Re^{p \times q_i}$ .In which $F_j = [F_{j1}, ... F_{j2}, ... F_{jq_j}] \in \Re^{p \times q_i}$. Further, in each of the training faces, the dimensions are defined as p and the count of the training face image is denoted as jq_j (from class j), and $q = \sum_{j=1}^{j=c} q_j$. $\mathrm{B} \in \Re^{p \times d}$ and $d < p$ represent the subspace projection matrix that has to be learned. The mapping of each of f_{ji} on to the learned subspace is denoted as $g_{ji} = \mathrm{B}^T f_{ji}$, in which $1 \le i \le q_j$.

The overall facial training image is mapped as $G = \mathrm{B}^T F \in \Re^{d \times q}$ and for every class $G_j = \mathrm{B}^T F_j \in \Re^{d \times q_j}$ .The CBCRE and WCRE are defined as in Eq. (9).

$$CBCRE = \frac{1}{q}\sum_{j=1}^{c}\sum_{i=1}^{q_j} \| g_{ji} - \hat{g}_{ji}^{inter} \|_2^2$$

$$WCRE = \frac{1}{q}\sum_{j=1}^{c}\sum_{i=1}^{q_j} \| g_{ji} - \hat{g}_{ji}^{intra} \|_2^2 \quad (9)$$

Where $\hat{g}_{ji}^{inter} = G_{ji}^{inter} \alpha_{ji}^{inter}$ and $\hat{g}_{ji}^{intra} = G_{ji}^{intra} \alpha_{ji}^{intra} \cdot G_{ji}^{inter}$ is G with G_i eliminated and G_{ji}^{intra} is G_j with g_{ji} eliminated. α_{ji}^{inter} and α_{ji}^{intra} is attained by Eq. (10).

$$\hat{\alpha}_i = \left(F_j^T F_j\right)^{-1} F_j^T g, j = 1,2,..g \quad (10)$$

The value of α is unknown before obtaining B in the learned subspace [26]. However, in the original space the value of $\hat{\alpha}$ is evaluated and $\hat{\alpha}$ is used as the approximation of α. According to the CBCRE concept given in Eq. (9), CBCRE and BCRE differ in that CBCRE employs cross-class collaborative representation while BCRE employs class-specific representation. Further, the relation existing in F and G, the WCRE and CBCRE can be written as per Eq. (11)

$$\begin{aligned} CBCRE &= \sum_{j=1}^{c}\sum_{i=1}^{q_j} \| \mathrm{B}^T f_{ji} - \mathrm{B}^T F_{ji}^{inter} \alpha_{ji}^{inter} \|_2^2 \\ WCRE &= \sum_{j=1}^{c}\sum_{i=1}^{q_i} \| \mathrm{B}^T f_{ji} - \mathrm{B}^T F_{ji}^{intra} \alpha_{ji}^{intra} \|_2^2 \end{aligned} \quad (11)$$

This is again rewritten as in Eq. (12).

$$\begin{aligned} CBCRE &= \sum_{j=1}^{c}\sum_{i=1}^{q_j} \left(f_{ji} - F_{ji}^{inter} \alpha_{ji}^{inter}\right)^T \mathrm{B}\mathrm{B}^T \left(f_{ji} - F_{ji}^{inter} \alpha_{ji}^{inter}\right) \\ WCRE &= \sum_{j=1}^{c}\sum_{i=1}^{q_j} \left(f_{ji} - F_{ji}^{intra} \alpha_{ji}^{intra}\right)^T \mathrm{B}\mathrm{B}^T \left(f_{ji} - F_{ji}^{intra} \alpha_{ji}^{intra}\right) \end{aligned} \quad (12)$$

In the above tow cases (CBCRE and WCRE), the factor $\frac{1}{q}$ is common, and so it can be eradicated in a safer manner. The relative worth of CBCRE versus WCRE is not impacted by this safer eradication. As a result, Eq. (13) is used to represent the CBCRE and WCRE [26].

$$\begin{aligned} CBCRE &= \sum_{j=1}^{c}\sum_{i=1}^{q_j} tr\left(\mathrm{B}^T \left(f_{ji} - F_{ji}^{inter} \alpha_{ji}^{inter}\right)\left(f_{ji} - F_{ji}^{inter} \alpha_{ji}^{inter}\right)^T \mathrm{B}\right) \\ WCRE &= \sum_{j=1}^{c}\sum_{i=1}^{q_j} tr\left(\mathrm{B}^T \left(f_{ji} - F_{ij}^{intra} \alpha_{ji}^{intra}\right)\left(f_{ji} - F_{ji}^{intra} \alpha_{ji}^{intra}\right)^T \mathrm{B}\right) \end{aligned} \quad (13)$$

Here, $tr(\cdot)$ → trace operator

The eigen vectors J_b and J_w is denoted as in Eq. (14). Eventually, the CBCRE and WCRE are rewritten as in Eq.(15).

$$\begin{aligned} J_b &= \frac{1}{q}\sum_{j=1}^{c}\sum_{i=1}^{q_j} \left(f_{ji} - F_{ji}^{inter} \alpha_{ji}^{inter}\right)\left(f_{ji} - F_{ji}^{inter} \alpha_{ji}^{inter}\right)^T \\ J_w &= \frac{1}{q}\sum_{j=1}^{c}\sum_{i=1}^{q_j} \left(f_{ji} - F_{ji}^{intra} \alpha_{ji}^{intra}\right)\left(f_{ji} - F_{ji}^{intra} \alpha_{ji}^{intra}\right)^T \end{aligned} \quad (14)$$

$$\begin{aligned} CBCRE &= tr\left(\mathrm{B}^T J_b \mathrm{B}\right) \\ WCRE &= tr\left(\mathrm{B}^T J_w \mathrm{B}\right) \end{aligned} \quad (15)$$

The MMC is deployed to simultaneously maximize CBCRE and minimize WCRE. This is expressed as per Eq. (16).

$$\begin{aligned} \max_{\mathrm{B}} S(\mathrm{B}) &= \max_{\mathrm{B}} \left(CBCRE - WCRE\right) \\ &= \max_{\mathrm{B}} \left(tr\left(\mathrm{B}^T \left(J_b - J_w\right)\mathrm{B}\right)\right) \end{aligned} \quad (16)$$

The mathematical expression given in Eq. (16) is solved by means of determining the largest d eigen values and the associated eigenvalues according to Eq (17).

$$\left(J_b - J_w\right) b_k = \lambda_k b_k, \; k = 1,2....d \quad (17)$$

Here, $\lambda_1 \geq ..... \geq \lambda_k .....\lambda_d$ and $\mathrm{B} = [b_1,....b_k,...., b_d]$. The the SSSP, in which the face image dimension is larger than the training face images can be solved by MNC.

The comprehensive algorithm of LCDRC is summarized in the subsequent section:

1. A unit l_2 norm is acquired by normalizing all the training as well as testing face images.
2. The projection matrix B is found for the given training facial image F. Further, F is projected into the discriminant subspace in order to acquire $G = \mathrm{B}^T.F$.
3. For every class $j = 1,2,..,c$, the hat Matrix H_j is computed.
4. Then, for the specified test face image f, convert f into discriminant subspace by using Eq. (18). Then, for j^{th} class, the reconstruction is computed as per Eq. (19).

$$g = \mathrm{B}^T.f \quad (18)$$

$$\hat{g} = H_j.g_j \; ; j = 1,2,.., c \qquad (19)$$

5. Evaluate RC from j^{th} class: $e_j = \| g - \hat{g}_j$, $j = 1,2,..c$. The class with the lowest RC is assigned to the test face picture g.

This is a step in the LCDRC classification strategy where the retrieved features are multiplied by the project matrix according to Eq. (20). To improve the recognition accuracy, an unique optimization approach called CWLM is used to optimize the project matrix.

$$\mathrm{M} = F \times \mathrm{B} \qquad (20)$$

V. Hybrid Optimization Algorithm For Projection Matrix optimization : Objective Function and Solution Encoding

A. Objective Function and Solution Encoding

For the best tuning, the suggested model is given the project matrix as input. Fig. 2 provides an illustration of the solution encoding.

Solution Encoding

The major objective of the recommended facial recognition model is to minimize estimation error and predicted outcomes of the classifier. The objective method is mathematically expressed in Eq. (21) and the fitness function is expressed in Eq. (22).

$$error = (act - pred) \qquad (21)$$

$$FT = Min\left(Sum(error) + \lambda * \sum_{j=1}^{B_N} (\mathrm{B})^2 \right) \qquad (22)$$

Here, λ →regularization constant

B. Proposed Hybrid Model:

A new improved version of the method is provided in this work to improve the performance of the conventional WOA [27] algorithm and LA [32] [33] [34] [35] algorithm with regard to convergence rate and speed. According to reports, hybrid optimization methods [36] show promise for a number of search issues. The mathematical model of the CWLM algorithm is discussed here.

Step 1: Overall population (Pop) of solutions is initialized (WOA and LA).

Step 2: Find the fitness (Fit) of the overall population

Step 3: If $i <= Pop/5$, then update the solutions using the exploration phase of WOA expressed in Eq. (23).

$$\vec{X}_{(t+1)} = \left| \vec{X}_{rand} - \vec{V}.\vec{U} \right| \qquad (23)$$

Here, the random position vector selected is denoted as $X_{(rand)}$. Further, $\vec{V}$ is a random value in the interval $[-v, v]$, in which v decreasing from 0 to 2.

Step 4: Else If $i <= Pop/5 \,\&\&\, i <= 2Pop/5$, then update the solutions using prey encircling phase of WOA. This is mathematically expressed in Eq. (24) and Eq. (25), respectively.

$$.\vec{U} = \left| \vec{C}.\vec{X}_{p(t)} - \vec{X}_{(t)} \right| \qquad (24)$$

$$\vec{X}_{(t+1)} = \vec{X}_{p(t)} - \vec{V}..\vec{U} \qquad (25)$$

In which, $\vec{V}$ and $.\vec{U}$ are the coefficient vectors. The letter t stands for the current iteration. Additionally, $\vec{X}_p$ and $\vec{X}$ is the best location of the best outcomeacquired and position vector, respectively.

Step 5: Else If $i <= 2Pop/5 \,\&\&\, i <= 3Pop/5$, then modify the solution's tri-level spiral evaluation position under the bubble net attack plan. Eq. (26) provides a mathematical formulation for this

$$X_{(t+1)} = \vec{U}' e^{bl}.Cos(2\pi l) + \vec{X}_{p(t)} \qquad (26)$$

The mathematical formula for $\vec{U}'$ is expressed in Eq. (27). Here, $\vec{U}'$ is the distance of i^{th} whale to prey and b is a constant that defines logarithm helical form. In addition, random number l is in between the range $[-1,1]$

$$\vec{D}' = \left| \vec{X}_{p(t)} - \vec{X}_{(t)} \right| \quad (27)$$

Step 6: Else if $i <= 3Pop/5 \&\& i <= 4Pop/5$. Then update the position of solutions using the mutation process of LA.

Step 7: The female version of LA, as described in Equations (28) and (29), is applied to the remaining solutions.

$$x_l^{Fe+} = \min\left[x_u^{\max}, \max(x_u^{\min}, \nabla_u)\right] \quad (28)$$

$$\nabla_u = \left\lfloor x_u^{Fe} + (0.1r_2 - 0.05)(x_u^{Ma} - r_1 x_u^{Fe}) \right\rfloor \quad (29)$$

On the other hand, when $Se_r > Se_r^{\max}$, the lioness X^{Fe} undergoes update X^{Fe+}. This process continues until gen_c (female generation count) reaches $gen_c^{\max}$. The mathematical formula for x_l^{Fe+} and x_u^{Fe+} corresponding to l^{th} and u^{th} vector element are denoted are expressed in Eq. (28) and Eq. (29), respectively. The female update function (∇) is expressed in Eq. (29). Here, r_2 and r_1 are integers.

Step 8: Subsequently, $Fit(i) = value(least\ fitness)$ is checked. Among the overall population, the position of least four fitness is evaluated. If these four fitness values lie within the aforementioned conditions (Step 3 – step 7), then the solution gets updated using Eq. (30). Here, $X^{\min}$ and $X^{\max}$ are the minimal and maximal boundaries of the output. In addition, ran is a random number.

$$X = X^{\min} + X^{\max} - X^{\min} * ran \quad (30)$$

Step 9: Terminate.

VI. RESULTS AND DISCUSSIONS

Simulation procedure

The suggested facial recognition method with optimization method was put into practice in MATLAB, and the outcome is documented. The ORL face dataset, Yale face dataset, and Face 94 dataset are three common databases from which the evaluation's dataset was compiled. The database encompasses both male and female images. Figure 4 displays the example picture that was gathered for analysis. The suggested work is compared to other conventional methods like LCDRC-WOA [27], LCDRC [26] and LCDRC-CEWO [28] in terms of accuracy, FPR and FDR. By changing the regularization constant and learning percentage, this evaluation is conducted. Equations (27), (28), and (29), respectively, are the mathematical formulas for accuracy, FPR, and FDR.

$$\text{Accuracy} = \text{Correct predictions} / \text{Total predictions} = \frac{TrP + TrN}{TrP + TrN + FrP + FrN} \quad (27)$$

$$\text{FPR} = \frac{FrP}{FrP + TrN} \quad (28)$$

$$\text{FDR} = \frac{FrP}{FrP + TrP} \quad (29)$$

Here, TrP→True Positive, TrN→ True Negative, FrP→ False Positive, FrN→ False Negative

Overall Performance Evaluation: The performance metrics of four different models (LCDRC, LCDRC-WOA, LCDRC-CEWO, and LCDRC-CWLM) across various evaluation criteria. Let's analyse and compare the models based on the provided metrics:

The table presents the performance metrics of four different models (LCDRC, LCDRC-WOA, LCDRC-CEWO, and LCDRC-CWLM) across various evaluation criteria. Let's analyze and compare the models based on the provided metrics:

- Accuracy:
  - All models demonstrate high accuracy, with LCDRC-CWLM having the highest accuracy (0.98678).
- Sensitivity (True Positive Rate):
  - Sensitivity measures the proportion of actual positive cases correctly identified by the model.
  - LCDRC-WOA and LCDRC-CEWO exhibit the highest sensitivity (0.80263 and 0.81579, respectively).

- Specificity (True Negative Rate):
  - Specificity measures the proportion of actual negative cases correctly identified by the model.
  - All models have high specificity, with LCDRC-CWLM having the highest (0.98838).
- Precision:
  - Precision is the ratio of true positive predictions to the total predicted positives.
  - LCDRC-CWLM has the highest precision (0.29825).
- False Positive Rate (FPR):
  - FPR is the proportion of actual negative cases incorrectly classified as positive.
  - All models have low FPR, with LCDRC-CWLM having the lowest (0.011618).
- False Negative Rate (FNR):
  - FNR is the proportion of actual positive cases incorrectly classified as negative.
  - LCDRC-WOA has the lowest FNR (0.19737).
- Negative Predictive Value (NPV):
  - NPV is the ratio of true negative predictions to the total predicted negatives.
  - All models exhibit high NPV.
- False Discovery Rate (FDR):
  - FDR is the proportion of false positives among the predicted positives.
  - LCDRC-CWLM has the lowest FDR (0.70175).
- F1-score:
  - The F1-score is the harmonic mean of precision and sensitivity.
  - LCDRC-CWLM achieves the highest F1-score (0.42607).
- Matthews Correlation Coefficient (MCC):
  - MCC combines various metrics into a single value, considering both false positives and false negatives.

- LCDRC-CWLM has the highest MCC (0.46654).

In summary, table 1 describes the LCDRC-CWLM model which generally outperforms the other models across multiple metrics, indicating its overall superior performance in terms of accuracy, precision, F1-score, and MCC. However, the choice of the best model may depend on the specific priorities and requirements of the application, as different metrics emphasize different aspects of model performance.

In summary, LCDRC-CWLM generally outperforms the other models shown in fig 3 across multiple metrics, indicating its overall superior performance in terms of accuracy, precision, F1-score, and MCC. However, the choice of the best model may depend on the specific priorities and requirements of the application, as different metrics emphasize different aspects of model performance. Similarly, the variation of the metrices is shown in fig 4.

TABLE I OVERALL PERFORMANCE EVALUATION FOR FACE94 DATSET

Metrics	LCDRC [26]	LCDRC-WOA [27]	LCDRC-CEWO [28]	LCDRC-CWLM
Accuracy	0.97569	0.98382	0.98417	0.98678
Sensitivity	0.73904	0.80263	0.81579	0.74561
Specificity	0.97726	0.98502	0.98528	0.98838
Precision	0.17709	0.26194	0.26854	0.29825
FPR	0.022743	0.014977	0.014715	0.011618
FNR	0.26096	0.19737	0.18421	0.25439
NPV	0.97726	0.98502	0.98528	0.98838
FDR	0.82291	0.73806	0.73146	0.70175
F1-score	0.28571	0.39498	0.40407	0.42607
MCC	0.35438	0.45307	0.46274	0.46654

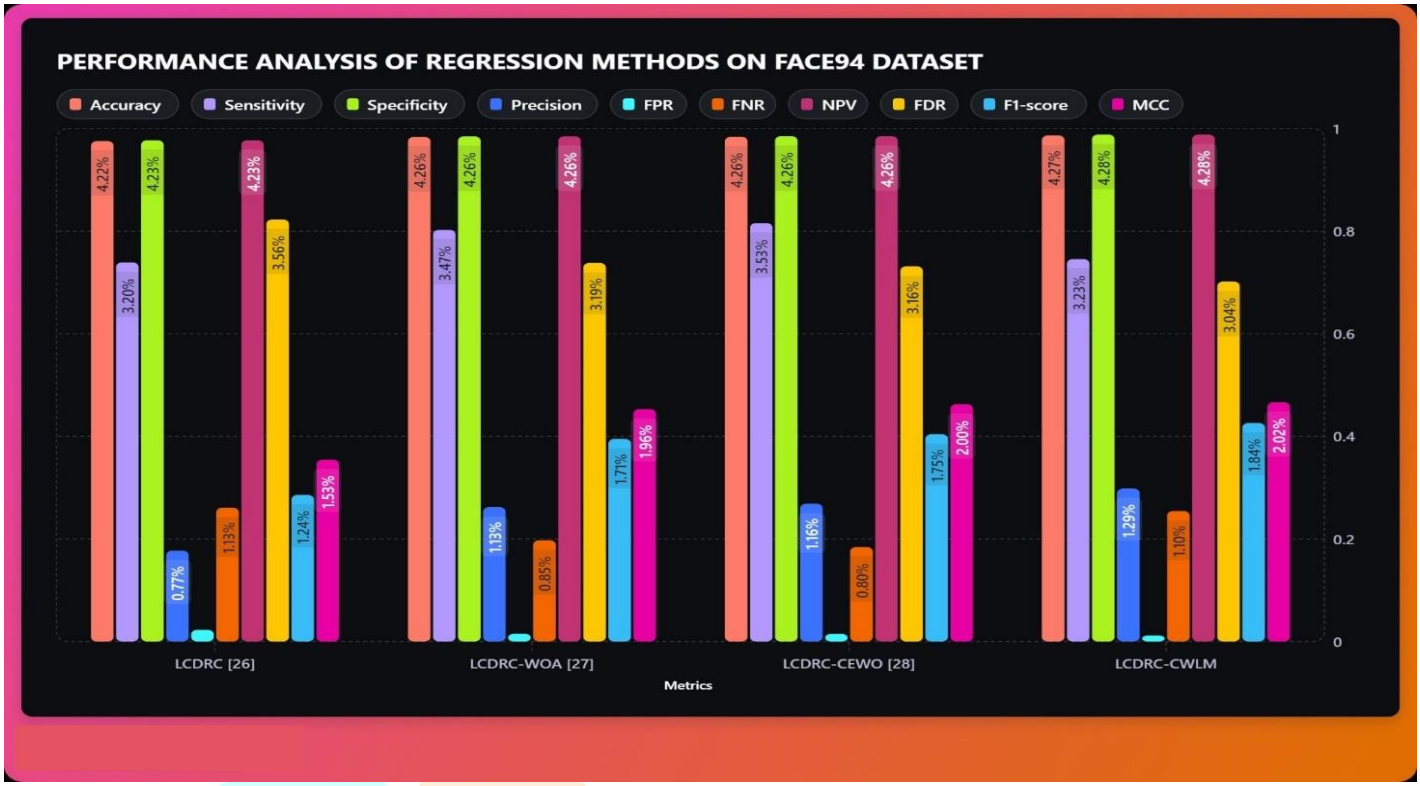

Fig 3: Performance measures on FACE94 Dataset using Regression Methods

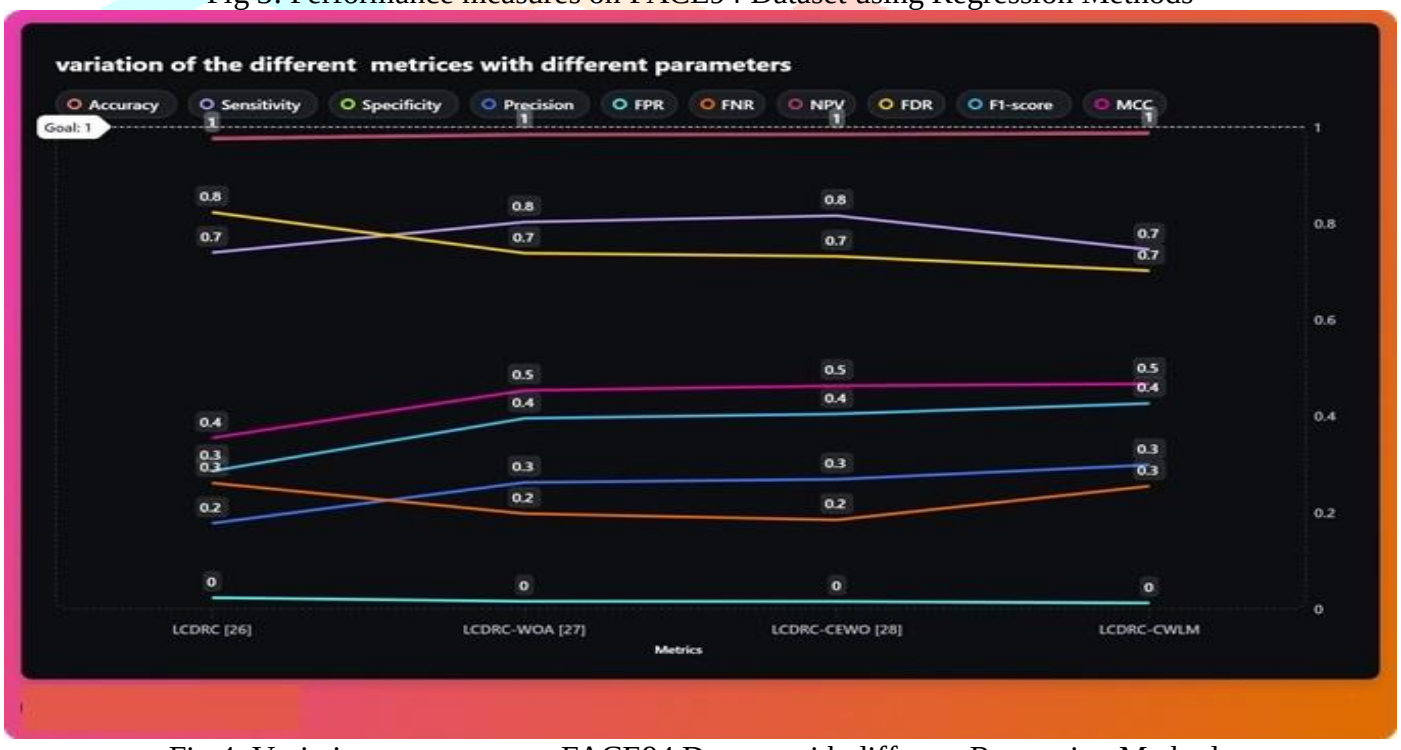

Fig 4: Variations measures on FACE94 Dataset with different Regression Methods

B.Performance Evaluation in terms of Accuracy: Varying the length of Attributes:

By adjusting the length of characteristics, the performance of the proposed work is compared to that of the current models LCDRC, LCDRC-WOA, and LCDRC-CEWO. Accuracy is considered in this rating. Figure 5 displays visually the comparable outcome obtained for the Face94, Yale, and ORL datasets. This shown in Fig 5(a) accuracy of the proposed work is 0.81 percent, 0.20 percent, and 0.10 percent better than LCDRC, LCDRC-WOA, and LCDRC-CEWO, respectively, for the Face94 dataset at attribute length 30. Furthermore, the accuracy of the provided work is the greatest when compared with existing ones, and at attribute length=11, it is 4.3%, 0.5%, and 1.03 percent better than LCDRC, LCDRC-WOA, and LCDRC-CEWO, respectively. This is shown in Fig. 5(b), which corresponds to the Yale dataset. The accuracy of the given and previous work for the ORL dataset is shown in Fig. 5(c). When compared to the previous work, the work that is being given here seems to be superior. The given work therefore appears to demonstrate a greater degree of accuracy based on the overall evaluation.

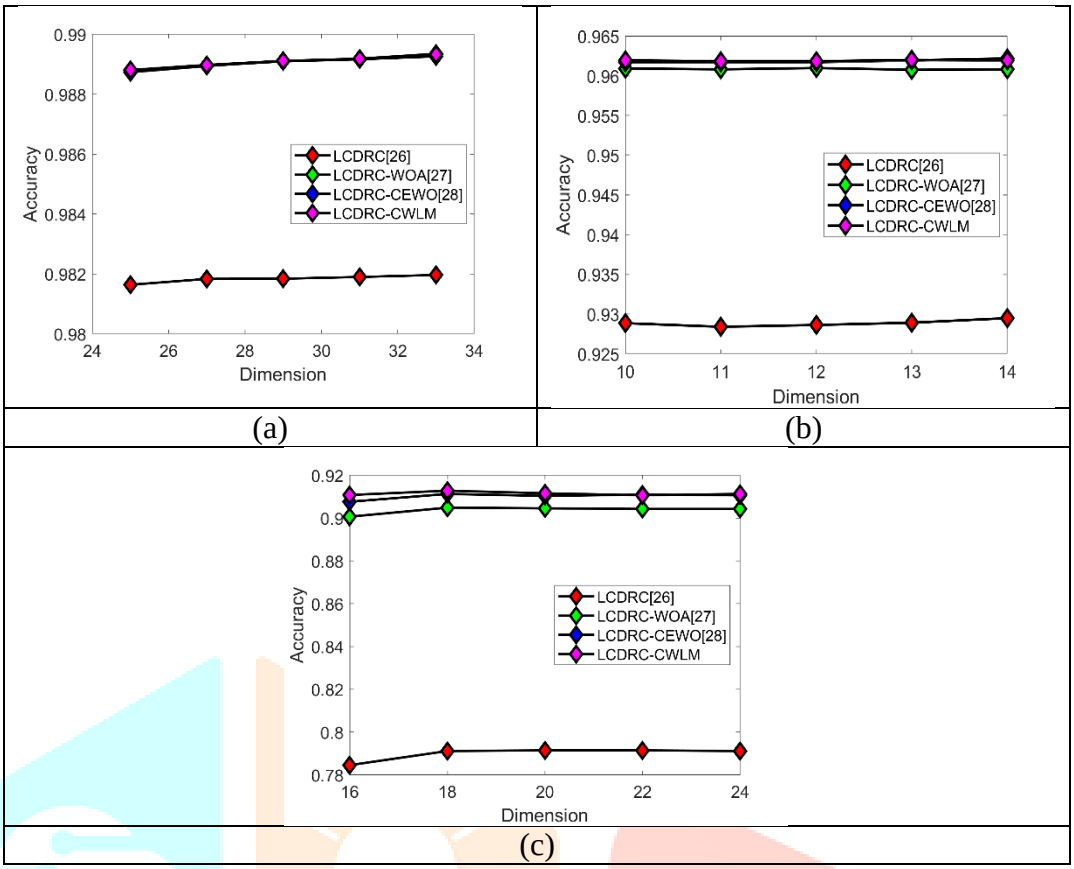

Fig 4 Performance evaluation of the presented work (LCDRC- CWLM) over the traditional approaches by means of varying the length of attributes for (a) Face 94 dataset, (b) Yale dataset and (c) ORL dataset

VI. CONCLUSION

This model introduces a ground-breaking face recognition system with three main steps: pre-processing, feature extraction, and classification. In the pre-processing phase, the facial image undergoes contrast enhancement and RGB to grayscale conversion. Texture characteristics are then extracted using Active Appearance Models (AAM). For classification, an optimized LCDRC model is employed, where the crucial assessment is the projection matrix. The matrix, multiplied with the extracted characteristics, plays a key role in the classification process. To enhance accuracy, a novel hybrid method called WOA-LA hybrid algorithm, combining WOA and LA (lion algorithm) concepts, is developed to improve the projection matrix. Performance is evaluated against other methods, such as LC-DRC, LCDRC-WOA, and LCDRC-CEWO, using metrics like Accuracy, False Positive Rate (FPR), and False Discovery Rate (FDR). The proposed model demonstrates competitive accuracy, particularly outperforming existing models at LP=80. Notably, for Face 94, the presented work consistently achieves higher accuracy than comparison models. Specifically, at tr-sample=2, the accuracy is 0.51%, 0.01%, and 0.03% better than LCDRC, LCDRC-WOA, and LCDRC-CEWO, respectively, with an overall accuracy of 98.82%.

REFERENCES

[1] R. He, J. Cao, L. Song, Z. Sun and T. Tan, "Adversarial Cross-Spectral Face Completion for NIR-VIS Face Recognition," in IEEE Transactions on Pattern Analysis and Machine Intelligence, vol. 42, no. 5, pp. 1025-1037, 1 May 2020, doi: 10.1109/TPAMI.2019.2961900.

[2] F. Liu, Q. Zhao, X. Liu and D. Zeng, "Joint Face Alignment and 3D Face Reconstruction with Application to Face Recognition," in IEEE Transactions on Pattern Analysis and Machine Intelligence, vol. 42, no. 3, pp. 664-678, 1 March 2020, doi: 10.1109/TPAMI.2018.2885995.

[3] C. Fu, X. Wu, Y. Hu, H. Huang and R. He, "DVG-Face: Dual Variational Generation for Heterogeneous Face Recognition," in IEEE Transactions on Pattern Analysis and Machine Intelligence, vol. 44, no. 6, pp. 2938-2952, 1 June 2022, doi: 10.1109/TPAMI.2021.3052549

[4] M. Luo, J. Cao, X. Ma, X. Zhang and R. He, "FA-GAN: Face Augmentation GAN for Deformation-Invariant Face Recognition," in IEEE Transactions on Information Forensics and Security, vol. 16, pp. 2341-2355, 2021, doi: 10.1109/TIFS.2021.3053460.

[5] J. Zhao, S. Yan and J. Feng, "Towards Age-Invariant Face Recognition," in IEEE Transactions on Pattern Analysis and Machine Intelligence, vol. 44, no. 1, pp. 474-487, 1 Jan. 2022, doi: 10.1109/TPAMI.2020.3011426.

[6] J. Chen, J. Chen, Z. Wang, C. Liang and C. -W. Lin, "Identity-Aware Face Super-Resolution for Low-Resolution Face Recognition," in IEEE Signal Processing Letters, vol. 27, pp. 645-649, 2020, doi: 10.1109/LSP.2020.2986942.

[7] J. Y. Choi and B. Lee, "Ensemble of Deep Convolutional Neural Networks With Gabor Face Representations for Face Recognition," in IEEE Transactions on Image Processing, vol. 29, pp. 3270-3281, 2020, doi: 10.1109/TIP.2019.2958404

[8] H. Yang and X. Han, "Face Recognition Attendance System Based on Real-Time Video Processing," in IEEE Access, vol. 8, pp. 159143-159150, 2020, doi: 10.1109/ACCESS.2020.3007205.

[9] Leslie Rollins, Aubrey Olsen, Megan Evans, "Social categorization modulates own-age bias in face recognition and ERP correlates of face processing", Neuropsychologia, in communication,2020

[10] Fenggao Tang, Xuedong Wu, Zhiyu Zhu, Zhengang Wan, Lili Gu, "An end-to-end face recognition method with alignment learning",Optik, vol.205,March 2020

[11] Bozana Meinhardt-Injac, David Kurbel, Günter Meinhardt, "The coupling between face and emotion recognition from early adolescence to young adulthood", Cognitive Development, vol.53, January–March 2020

[12] Serign Modou Bah, Fang Ming,"An improved face recognition algorithm and its application in attendance management system",Array, vol.5,March 2020

[13] Mackenzie A. Sunday, Parth A. Patel, Michael D. Dodd, Isabel Gauthier,"Gender and hometown population density interact to predict face recognition ability",Vision Research, vol.163,pp.14-23,October 2019

[14] Guangwei Gao, Yi Yu, Meng Yang, Pu Huang, Dong Yue,"Multi-scale patch based representation feature learning for low-resolution face recognition",Applied Soft Computing,vol.90,May 2020

[15] Nesrine Grati, Achraf Ben-Hamadou, Mohamed Hammami,"Learning Local Representations for Scalable RGB-D Face Recognition", Expert Systems with Applications, in communication,2020

[16] Mehedi Masud, Ghulam Muhammad, Hesham Alhumyani, Sultan S Alshamrani, M. Shamim Hossain,"Deep learning-based intelligent face recognition in IoT-cloud environment",Computer Communications, vol.152,pp. 215-222,February 2020

[17] Shigang Liu, Yuhong Wang, Xiaosheng Wu, Jun Li, Tao Lei,"Discriminative dictionary learning algorithm based on sample diversity and locality of atoms for face recognition",Journal of Visual Communication and Image Representation, in comunication,2020

[18] Mingyu You, Xuan Han, Yangliu Xu, Li Li,"Systematic evaluation of deep face recognition methods",Neurocomputing, in communication,2020

[19] Ching Yiu Jessica Liu, Caroline Wilkinson,"Image conditions for machine-based face recognition of juvenile faces",Science & Justice, vol.60,no.1,pp.43-52,January 2020

[20] Mei Wang, Weihong Deng,"Deep face recognition with clustering based domain adaptation", Neurocomputing, in communication,2020

[21] Wenbo Zheng, Chao Gou, Fei-Yue Wang,"A novel approach inspired by optic nerve characteristics for few-shot occluded face recognition",Neurocomputing, vol.376,pp.25-41, February 2020

[22] Abdulaziz Zam, Mohammad Reza Khayyambashi, Ali Bohlooli,"Energy-efficient face detection and recognition scheme for wireless visual sensor networks",Applied Soft Computing, vol.89,April 2020

[23] Jingna Sun, Yehu Shen, Wenming Yang, Qingmin Liao,"Classifier shared deep network with multi-hierarchy loss for low resolution face recognition",Signal Processing: Image Communication, vol.82,March 2020

[24] Ben-Bright Benuwa, Benjamin Ghansah, Ernest K. Ansah, "Kernel based locality – Sensitive discriminative sparse representation for face recognition",Scientific African, vol.7,March 2020

[25] Guodong Guo, Na Zhang, "A survey on deep learning-based face recognition", Computer Vision and Image Understanding, vol.189, December 2019

[26] Xiaochao Qu, Suah Kim, Run Cui and Hyoung Joong Kim, “z,” Visual communication image retrieval, vol. 31, pp. 312-319, 2015.

[27] Seyedali Mirjalili and Andrew Lewis, " The Whale Optimization Algorithm", Advances in Engineering Software, vol. 95, pp.51–67, 2016.

[28] Syed Akheell,"Cyclic Exploration-based Whale Optimization to Linear Collaborative Discriminant Regression Classification for Face Recognition", in communication

[29] R. Kaur and S. Kaur, "Comparison of contrast enhancement techniques for medical image," 2016 Conference on Emerging Devices and Smart Systems (ICEDSS), Namakkal, pp. 155-159,2016.

[30] K. Padmavathi1and K. Thangadurai, " Implementation of RGB and Grayscale Images in Plant Leaves Disease Detection – Comparative Study", Indian Journal of Science and Technology, vol. 9, no. 6, 2016.

[31] Y. H. Lee, W. Han, Y. Kim and B. Kim, "Facial Feature Extraction Using an Active Appearance Model on the iPhone," 2014 Eighth International Conference on Innovative Mobile and Internet Services in Ubiquitous Computing, Birmingham, pp. 196-201, 2014.

[32] Rajakumar Boothalingam, "Optimization using lion algorithm: a biological inspiration from lion’s social behavior", Evolutionary Intelligence, vol.11, no. 1-2, pp.31–52, 2018.

[33] B. R. Rajakumar, “Lion algorithm for standard and large-scale bilinear system identification: A global optimization based on Lion's social behavior”, 2014 IEEE Congress on Evolutionary Computation, Beijing, China, July 2014, pages: 2116-2123, DOI: 10.1109/CEC.2014.6900561

[34] B. R. Rajakumar, "The Lion's Algorithm: A New Nature Inspired Search Algorithm", Procedia Technology-2nd International Conference on Communication, Computing & Security, Vol. 6, pages: 126-135, 2012, DOI: 10.1016/j.protcy.2012.10.016 (Elsevier)

[35] B. R. Rajakumar, “Lion algorithm and its Applications”, Frontier Applications of Nature Inspired Computation in Springer Tracts in Nature-Inspired Computing (STNIC), Springer, Editors: Mahdi Khosravy, Neeraj Gupta, Nilesh Patel, Tomonobu Senju